PHYSICAL REVIEW B **87**, 060504(R) (2013)

Manipulating Majorana fermions in quantum nanowires with broken inversion symmetry

Xiong-Jun Liu and Alejandro M. Lobos
Joint Quantum Institute and Condensed Matter Theory Center, Department of Physics, University of Maryland, College Park, Maryland 20742, USA

(Received 11 July 2012; revised manuscript received 12 December 2012; published 15 February 2013)

We study a Majorana-carrying quantum wire, driven into a trivial phase by breaking the spatial inversion symmetry with a tilted magnetic field. Interestingly, we predict that a supercurrent applied in the proximate superconductor is able to restore the topological phase and therefore the Majorana end states. Using Abelian bosonization, we further confirm this result in the presence of electron-electron interactions and show a profound connection of this phenomenon to the commensurate-incommensurate transition in one-dimensional doped Mott insulators. These results have important applications in, e.g., realizing a supercurrent-assisted braiding of Majorana fermions, which proves highly useful in topological quantum computation with realistic Majorana networks.

DOI: 10.1103/PhysRevB.87.060504 PACS number(s): 71.10.Pm, 74.45.+c, 74.78.Na, 03.67.Lx

The study of topological superconductors (SCs) which host Majorana zero bound states (MZBSs) has developed into a rapidly growing branch of condensed matter physics, driven by both the pursuit of exotic fundamental physics and the applications in fault-tolerant topological quantum computation (TQC).[1–3] The MZBS exists in the vortex core of a two-dimensional (2D) $(p+ip)$-wave SC,[4] and at the ends of a 1D p-wave SC.[5,6] However, intrinsic p-wave superconductivity is not necessary to observe the MZBS: Recent proposals have shown the equivalence of topological insulator/s-wave SC heterostructures[7–9] and spin-orbit (SO) coupled semiconductor/s-wave SC heterostructures with Zeeman splitting[10–16] to p-wave SCs. In such devices, the SO interaction drives the original s-wave SC into an effective p-wave SC, leading to MZBSs in the case of odd number of subbands crossing the Fermi level. It has been predicted that an isolated MZBS can induce a zero-bias peak (ZBP) of height $2e^2/h$ (at zero temperature) in the differential tunneling conductance dI/dV at the interface with a normal contact.[17–21] Recent experiments in semiconducting nanowires (NWs)/s-wave SC heterostructures have shown a suggestive ZBP in the dI/dV spectra,[22–25] which disappears when the external magnetic field is tilted from the direction of the NW and eventually aligned in the quantization axis of the SO coupling.[22,24]

Motivated by these recent findings, in this Rapid Communication we investigate a Majorana quantum NW driven into the trivial phase by a tilted magnetic field which breaks 1D spatial inversion symmetry (SIS),[20] as observed in the experiments.[22,24] Quite interestingly, we show that a supercurrent applied in the SC can compensate for the detrimental effects of the tilted magnetic field, therefore restoring the MZBS. Using Abelian bosonization we show the robustness of these results in the presence of electron-electron (e-e) interaction, and find a profound connection to the physics of doped 1D Mott insulators and the commensurate-incommensurate transition (CICT).[26] We finally propose a supercurrent-assisted braiding (SAB) of MZBSs, which may have important applications in TQC with realistic Majorana networks.

We start from the model of a 1D SO-coupled NW in proximity to an s-wave SC, with a Zeeman field $\vec{V}=(V_x,V_y)=V_0(\cos\theta,\sin\theta)$ given by an external magnetic field tilted from the NW by an angle θ. For $\theta=0$, a phase transition from a trivial to a topological SC occurs by tuning V_0 to be $V_0>(\mu^2+|\Delta_s|^2)^{1/2}$,[10,11,27] where μ and Δ_s are the chemical potential and induced s-wave SC order parameter in the NW, respectively. The Hamiltonian of the system reads $H=H_0+H_s$, where

$$\begin{aligned} H_0 &= \int dx\,\mathbf{c}^\dagger(x)\left[\frac{\partial_x^2}{2m^*}-\mu+i\lambda_R\boldsymbol{\sigma}_y\partial_x+\vec{V}\cdot\vec{\boldsymbol{\sigma}}\right]\mathbf{c}(x),\\ H_s &= \int dx[\Delta_s c_\uparrow(x)c_\downarrow(x)+\text{H.c.}], \end{aligned} \tag{1}$$

with $\mathbf{c}(x)=[c_\uparrow(x),c_\downarrow(x)]$ the electron annihilation field operator, m^* the effective mass of electrons in the NW, λ_R the Rashba SO coupling coefficient, and $\vec{\boldsymbol{\sigma}}=(\boldsymbol{\sigma}_x,\boldsymbol{\sigma}_y,\boldsymbol{\sigma}_z)$ the vector of Pauli matrices. The term $V_y\sigma_y$, occurring due to a finite tilt angle θ, breaks SIS of the NW.[20] This can be seen directly in H_0 under the 1D space-inversion transformation $x\to -x$, $(y,z)\to(y,z)$, which leads to $(k,\sigma_y)\to(-k,-\sigma_y)$ and $\sigma_x\to\sigma_x$, with k the momentum in NW. The broken SIS leads to an asymmetric dispersion relation $\varepsilon_k^{(\pm)}\neq\varepsilon_{-k}^{(\pm)}$ for H_0.[28] Accordingly, the Bogoliubov quasiparticle spectra with a uniform Δ_s are also asymmetric $E(k)\neq E(-k)$ [Fig. 1(a)]. In particular, when θ exceeds a critical value $\theta_c(V_0,\Delta_s,\mu)$, the broken SIS closes the bulk gap and a finite Fermi surface is obtained [red dashed curves in Fig. 1(a)]. This drives the system into a trivial SC for $\theta>\theta_c$.

We proceed to show that the topological phase can be restored at $\theta>\theta_c$ by a supercurrent J_s applied in the proximate SC. A uniform J_s induces a position-dependent phase in Δ_s as $\Delta_s(x)=|\Delta_s|e^{i\phi(x)}$, related to the supercurrent through $J_s=2n_se\hbar\alpha[1-(\alpha\xi)^2]/m_e$,[31] with $\alpha=\nabla\phi(x)$ a uniform phase gradient, and m_e, n_s, and ξ the electron mass, superconducting carrier density, and coherence length in the bulk SC, respectively. The applied J_s should be less than the superconducting critical current $J_c=4n_se\hbar/(3\sqrt{3}m_e\xi)$.[31] The physics of the problem can be seen more transparently by projecting H onto the lower subband of the NW, $H\approx H^{(-)}=\sum_k[\varepsilon_k^{(-)}-\mu]c_{k,-}^\dagger c_{k,-}+\frac{1}{2}\sum_k[\Delta_s e^{i\chi_k}c_{k,-}c_{-k-\alpha,-}+\text{H.c.}]$, where $\chi_k=\tan^{-1}[(V_y-\lambda_Rk)/V_x]$ and $\varepsilon_k^{(-)}>\varepsilon_{-k}^{(-)}$ for $k>0$ and $0<\theta<\pi$. For $J_s=0$, electron states with opposite momenta $\pm k$ are

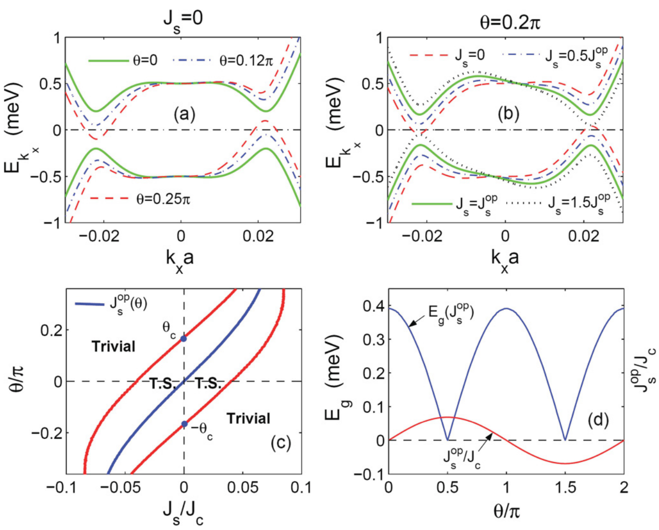

FIG. 1. (Color online) (a) Vanishing of the bulk gap by increasing tilt angle θ. (b) Restoring of the bulk gap at $\theta = 0.2\pi$ by applying supercurrents. (c) Phase boundary between topological superconducting (T.S.) and trivial phases with a supercurrent. (d) Superconducting bulk gap vs optimal supercurrent. Parameters are taken according to Ref. 22: $V_0 = 1.0$ meV, $\Delta_s = 0.5$ meV, $\mu = 0$, and SO energy $E_{\rm so} = m^*\lambda_R^2 = 0.1$ meV (a)–(d), resulting in a critical angle $\theta_c \approx 0.168\pi$ (cf. also Ref. 30).

off resonant and the formation of Cooper pairs with zero center-of-mass momentum is weakened. For a supercurrent applied along the $+x$ direction (i.e., $\alpha > 0$), the Hamiltonian pairs up states with momenta k and $-k-\alpha$ which are closer in energy, favoring the formation of a Cooper pair with center-of-mass momentum α. A supercurrent therefore allows to compensate for the band asymmetry induced by the tilted magnetic field, strengthening the bulk gap in the NW.

In Fig. 1(b) we show that the bulk gap, which vanishes for $\theta = 0.2\pi$ at $J_s = 0$, reopens in the presence of J_s in the $+x$ direction, and attains its maximum at the optimal value $J_s = J_s^{\rm op}$ (green solid line). Further increasing J_s suppresses again the bulk gap due to an over compensation of the band asymmetry and induces again an off-resonant situation (black dotted line). Our results are summarized in Fig. 1(c), which shows the phase diagram of the NW as a function of J_s and θ, with $\xi \leqslant 10$ nm the typical coherence length in NbTi SCs.[32] The blue curve represents the optimal supercurrent $J_s^{\rm op}(\theta)$, and the red curves give boundaries of the topological and trivial phases. For $J_s = 0$, the phase becomes trivial when $\theta_c \leqslant |\theta| < \pi/2$, while applying a supercurrent along $+x$ (or $-x$, depending on the sign of θ) can restore the topological phase [Fig. 1(c)]. In contrast, for $\theta = 0$ the optimal supercurrent is $J_s^{\rm op} = 0$, and applying a J_s breaks the SIS and destabilizes the topological phase.[33] Figure 1(c) therefore provides a useful guide to explore systematically the topological phase diagram in ongoing experiments.[22–24] The bulk gap $E_g(J_s^{\rm op})$ versus $J_s^{\rm op}$ is given in Fig. 1(d), from which one finds a vanishing $E_g(J_s^{\rm op})$ only at $\theta = \pi/2, 3\pi/2$, indicating that MZBSs can always be restored by a supercurrent unless the magnetic field is perpendicular to NW.

To determine if the above results are robust against e-e interactions in the NW, we introduce here the Abelian bosonization framework. At low energies, linearizing the dispersion relation $\varepsilon_k^{(-)}$ around the Fermi energy E_F generates asymmetric left (right) Fermi momenta $k_{L(R)}$ and Fermi velocities $v_{L(R)}$ due to the broken SIS. We next introduce the standard bosonic representation of left/right-moving fermions $c_{L/R} \sim \frac{1}{\sqrt{2\pi a}} e^{i(\mp\varphi-\vartheta)}$, with bosonic fields φ,ϑ obeying the canonical commutation relation $[\varphi(x), \vartheta(x')] = i\pi\,\mathrm{sgn}(x'-x)/2$ and $a \sim k_F^{-1}$ the short-distance cutoff of the continuum theory.[26] Physically, the field $\varphi(x)$ represents slowly varying fluctuations in the electronic density $\delta\rho(x) = -\partial_x\varphi(x)/\pi$, and $\vartheta(x)$ is related to the phase of the SC order parameter through $c_R(x)c_L(x) \propto e^{i2\vartheta(x)}$. With a short-range interaction $H_{\rm int} = \pi U \int dx\, c_R^\dagger(x) c_R(x) c_L^\dagger(x) c_L(x)$ the low-energy Hamiltonian is given in bosonic representation by[34]

$$H = \int dx \left\{ \frac{vK}{2\pi}(\partial_x\vartheta)^2 + \frac{v}{2\pi K}(\partial_x\varphi)^2 + \frac{\eta v}{\pi}\partial_x\varphi\partial_x\vartheta + \frac{|\Delta_p|}{\pi a}\sin[2\vartheta(x) + (\alpha - \delta k_F)x] \right\}, \tag{2}$$

where e-e interactions are encoded in the Luttinger parameter $K = \sqrt{(1-2U/v)/(1+2U/v)}$, $v = (|v_L| + |v_R|)/2$, and $\Delta_p = \Delta_s \sin(\frac{\chi_{k_L} - \chi_{-k_R-\alpha}}{2})$ is the effective p-wave SC order parameter. The variables $\eta = (|v_L| - |v_R|)/(|v_L| + |v_R|)$ and $\delta k_F = k_L - k_R$ quantify the band asymmetry. When $\Delta_p = 0$, the above model describes a Luttinger liquid (LL) fixed point with asymmetric dispersion relation, i.e., right- and left-going 1D plasmon excitations traveling at different velocities.[35–37] As shown in Ref. 37, the asymmetric LL is a stable fixed point with a well-defined Luttinger parameter if $\eta^2 + (2U/v)^2 < 1$. In general, the SIS-breaking term $\sim\eta\partial_x\varphi\partial_x\vartheta$ tends to enhance the detrimental effects of the oscillatory factor $(\alpha - \delta k_F)x$ (see the Supplemental Material[34] for details). However, for typical parameters used in Fig. 1, one can verify that $\eta < 1\%$ with any θ, and then $\eta\partial_x\varphi\partial_x\vartheta$ is negligible in the following analysis. We also note that for semiconductor NW, the system is far away from the half-filling condition and the NW length $L \gg L_c \equiv |4(k_R + k_L)/2 - 2\pi/a|^{-1}$. Thus the umklapp term $\cos[4\phi - 2(k_R + k_L)x]$ strongly oscillates at length scales larger than L_c and averages out to zero.[38]

For a small Δ_p, the low-energy physics is captured by the perturbative renormalization-group (PRG) approach around the LL fixed point.[38–41] Implementing a standard PRG procedure that leaves invariant the LL Gaussian fixed point under the change in the short-distance cutoff $a(\ell) = a_0 e^\ell \to a(\ell + d\ell)$ (cf., e.g., Refs. 26 and 42) allows to obtain the RG-flow equations $dK/d\ell = y^2 J_0(\delta p a(\ell))$, $dy/d\ell = (2 - K^{-1})y$ and $dv/d\ell = -y^2 v K J_2(\delta p a(\ell))$, with $\delta p \equiv \alpha - \delta k_F$.[34] Here $J_n(z)$ is the nth order Bessel function of the first kind and $y \equiv \Delta_p a_0/v$ is a dimensionless perturbative parameter which becomes relevant (in the RG sense) for $K > 1/2$ and $\alpha = \delta k_F$.[38–41] Interestingly, our RG equations are analogous to those describing the CICT in doped 1D Mott-insulating systems after the rescaling $\tilde{K} = 4K, \tilde{\vartheta} = \vartheta/2, \tilde{\varphi} = 2\varphi$, and the subsequent duality transformation $\tilde{\vartheta} \leftrightarrow \tilde{\varphi}, \tilde{K} \leftrightarrow 1/\tilde{K}$.[43–45] The crucial term $\delta p x$ in Eq. (2) plays the role of the particle doping (relative to half-filling case) in the CICT, which has the effect of closing the Mott-insulating gap. Analogously, in our case a finite δp may close the

SC gap. The condition $\alpha = \delta k_F$ (i.e., $\delta p = 0$) determines the optimal supercurrent $\frac{J_s^{\rm op}}{J_c} = \frac{3\sqrt{3}}{2}[1-(\xi\delta k_F)^2]\xi\delta k_F$ in the bosonization approach, for which the topological phase is maximally restored. This result is independent of interactions, and relies on the linearization of $\varepsilon_k^{(-)}$ around E_F (nonlinearities may slightly correct $J_s^{\rm op}$).

We now estimate the critical value δp_c for the topological phase transition. If $\delta p a(\ell) \ll 1$, the sin function in Eq. (2) is weakly oscillating and the term $\delta p x$ can be dropped, rendering the RG equations similar to the those of the (undoped) sine-Gordon model.[38–41] In that case and for $K > 1/2$, we reach the strong-coupling regime $y(\ell^*) \sim 1$ at the scale $\ell^* = (2-K^{-1})^{-1}\ln(\xi_{\rm nw}/a_0)$ with $\xi_{\rm nw} = v/|\Delta_p|$. In this regime, the SC term $\Delta_p \sin 2\vartheta$ dominates in Eq. (2), and the value of $\vartheta(x)$ is pinned to the classical minima $\vartheta(x) = \{-\pi/4, 3\pi/4\}$, reflecting the underlying $\mathbb{Z}_2$ symmetry of the Majorana chain in the limit $L \to \infty$.[6,40,41] As δp increases, the regime $\delta p a(\ell) > 1$ is eventually reached and the sin function becomes strongly oscillating and averages to zero. At that point the above RG equations are no longer valid and the renormalization of $y(\ell)$ must be stopped.[26] The critical value δp_c can be estimated from the condition $\delta p_c a(\ell^*) = 1$, which implies that

$$\delta p_c \sim \frac{1}{a_0}\left(\frac{a_0}{\xi_{\rm nw}}\right)^{\nu}, \quad \nu = \frac{1}{2-K^{-1}}. \tag{3}$$

This is an important result in our work. In particular, the noninteracting case $U = 0$ (or $K = 1$) results in $\delta p_c \propto \xi_{\rm nw}^{-1} \propto \Delta_p$, which has been confirmed by direct numerical calculation in the noninteracting model. In the case $K \neq 1$, and for fixed $y_0 = y(\ell = 0)$, we observe that repulsive (attractive) *e-e* interaction destabilizes (stabilizes) the topological phase, inducing a smaller (larger) δp_c. Importantly, for $K > 1/2$ and tilt angle $|\theta| < \pi/2$, Eq. (3) implies that the topological phase can always be restored with a supercurrent such that $|\alpha - \delta k_F| < \delta p_c$.

Our results can be measured in the tunneling transport spectroscopy.[17–20] We consider a single normal metallic lead with a bias voltage eV_b, weakly coupled to the left end of the NW via the tunneling Hamiltonian $H_T = \sum_{p,q}' T_{p,q} d_p^\dagger \hat{c}_q + \sum_{p,j} T_{p,j} d_p^\dagger \gamma_j + \text{H.c.}$, where $T_{\mu\nu}$, d_p, and γ_j are the tunneling coefficients, the electron annihilation operator in metallic lead, and the Majorana operators at the left ($j = L$) and right ($j = R$) NW ends, respectively. The sum $\sum'$ runs over the 1D-bulk states in the NW, and $|T_{p,L}| \gg |T_{p,R}|$ due to the localization of Majorana modes. In the topological phase, both the MZBS and 1D-bulk continuum modes in the NW contribute to the tunneling current $I = -e\dot{N} = \frac{ie}{\hbar}[N, H_T]$, where $N = \sum_p d_p^\dagger d_p$. Using the Keldysh formalism and following Refs. 18 and 20 we obtain

$$\begin{aligned} I = {} & \frac{e^2}{h}\int d\omega\, \mathrm{Tr}[\Gamma^e \mathcal{G}^R(\omega)\Gamma^h \mathcal{G}^A(\omega)][1 - f(\omega - eV_b)] \\ & + \frac{e^2}{h}\int d\omega \Gamma(\omega) N(\omega)[1 - f(\omega - eV_b)], \end{aligned} \tag{4}$$

where $f(\omega)$ is Fermi distribution function and the trace is taken in the subspace spanned by γ_j modes. The retarded and advanced Majorana Green's functions $\mathcal{G}^R(\omega) = [\mathcal{G}^A(\omega)]^\dagger$ and

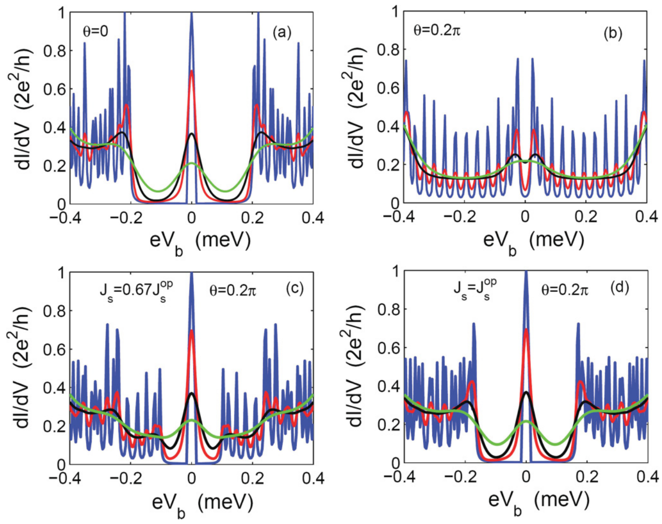

FIG. 2. (Color online) dI/dV for (a) $\theta = 0$ and (b) $\theta = 0.2\pi$ with $J_s = 0$. (c), (d) Restoring the ZBP at $\theta = 0.2\pi$ by supercurrents. The blue, red, black, and green curves correspond to the temperature $T = 0$, 60, 180, and 360 mK, respectively. Other parameters are $V_0 = 1.0$ meV, $E_{\rm so} = 0.1$ meV, $\Delta_s = 0.5$ meV, and the tunneling energies $|\Gamma_{LL}^{e,h}| \sim |\Gamma| = 0.005$ meV.

$[\mathcal{G}^R(\omega)]^{-1} = \omega/2 + i[\Gamma^e(\omega) + \Gamma^h(\omega)]/2$, where $\Gamma_{ij}^e(\omega) = \Gamma_{ij}^{h*}(-\omega) = 2\pi\sum_p T_{p,i}T_{p,j}^*\delta(\omega - \varepsilon_p)$ are the self-energies, and ε_p the single-electron dispersion relation in the metallic lead. The second term in the right hand side of Eq. (4) represents the contribution from 1D-bulk states, where $\Gamma(\omega) = 2\pi\sum_p |T_{p,q}|^2\delta(\omega - \varepsilon_p)$, and $N(\omega)$ is the 1D-bulk density of states in the NW.

Numerical results of dI/dV are plotted in Figs. 2(a)–2(d) at different temperatures. For $J_s = 0$, a ZBP is obtained when $\theta < \theta_c \approx 0.168\pi$ [Fig. 2(a)], and disappears when $\theta > \theta_c$ [Fig. 2(b)]. This result is consistent with the experimental observation in Ref. 22. Figures 2(c) and 2(d) show that the Majorana-carrying phase is restored by a finite supercurrent along the $+x$ direction at $\theta = 0.2\pi$, and maximizes at $J_s = J_s^{\rm op} \approx 0.039 J_c$ with $\xi \sim 10$ nm [Fig. 2(d)].[32] The ZBP in the dI/dV spectra is clearly restored, indicating the reemergence of the MZBS after the bulk SC gap reopens. Further increasing J_s again reduces the bulk gap [refer to Fig. 1(b)]. We confirm that the ZBP is $2e^2/h$ at $T = 0$, when the tunneling coefficients are small relative to the superconducting bulk gap, and is strongly suppressed by thermal broadening. The disappearance and restoration of the ZBP provide useful experimental tests for topological superconductivity in the laboratory.

Finally we propose an important application of our findings to braiding MZBSs, as needed in TQC. For a 1D system, the braiding operation in a single NW is not well defined, and the minimum requirement to exchange two MZBSs is to consider a T or Y junction composed of several NW segments.[46,47] A realistic 2D/3D network of MZBSs applicable for TQC can be constructed by putting together multiple NW junctions.[48] However, in such a network some of the NW segments are unavoidably misaligned with the external magnetic field $\boldsymbol{B}$, therefore breaking the SIS in those NWs. Thus, being able to drive all NWs deep into topological phase then becomes questionable, bringing an inevitable difficulty to braid MZBSs.

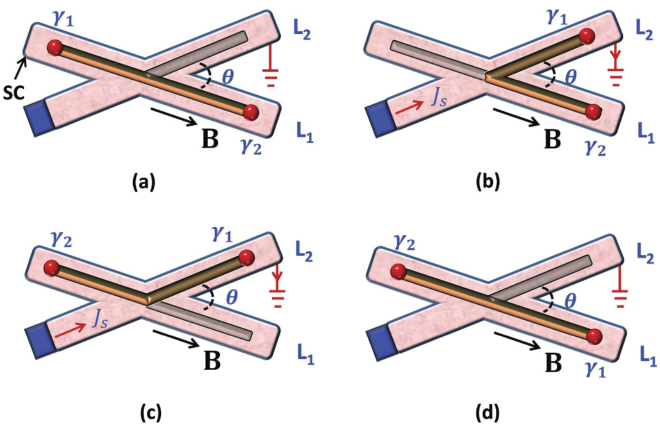

FIG. 3. (Color online) Supercurrent-assisted braiding (SAB) of two MZBS in a Y junction. (a) For $\theta > \theta_c$, the NW segment L_2 is initially in the trivial phase at $J_s = 0$. (b) Move the MZBS γ_1 to NW L_2 by applying a supercurrent $J_s = J_s^{\rm op}$ in L_2. (c) Move γ_2 to the original position of γ_1. (d) Move γ_1 to the NW L_1, and then turn off the supercurrent.

To resolve this problem, we introduce the SAB scheme, shown in Figs. 3(a)–3(d) for a Y junction. Here the spin quantization axis of a Rashba SO coupling is perpendicular to the NW and parallel to the SC plane (interface of the SC/NW heterostructure).[22] To minimize orbital effects, the $\boldsymbol{B}$ field must lie in the SC plane,[49] therefore breaking SIS for at least one of the two NW segments. If $\boldsymbol{B}$ is applied along the NW segment L_1 (Fig. 3), the segment L_2 is topologically trivial at $J_s = 0$ when $\theta > \theta_c$. On the other hand, to avoid the existence of low-energy excitations at the intersection of $L_{1,2}$, the tilt angle θ must be as close to $\pi/2$ as possible.[46] For the same parameters as in Fig. 1, the critical angle is $\theta_c \approx 0.168\pi$ (cf. also Ref. 30). Then for $\theta = 0.2\pi$, the NW L_2 is already in the trivial phase at $J_s = 0$ [Fig. 3(a)], and we next exchange $\gamma_{1,2}$ localized on the ends of L_1. To perform the braiding, we apply a $J_s = J_s^{\rm op} \approx 0.039 J_c$ along L_2 [with $\xi \sim 10$ nm for NbTi (Ref. 32)] and move adiabatically first γ_1 to NW L_2 by gate control [Fig. 3(b)]. Then we move γ_2 to the original position of γ_1 [Fig. 3(c)]. Finally γ_1 is shuttled to L_1, completing exchange with γ_2, and the supercurrent is turned off after braiding [Fig. 3(d)]. Note that supercurrent is needed only in the intermediate process of the braiding operation. Applying the SAB to generic 2D or 3D Majorana networks can provide vast flexibility for the realistic TQC with MZBS.

In summary, we have studied the disappearance and reemergence of MZBSs in Majorana quantum wires with broken SIS, under the simultaneous effects of a tilted magnetic field and supercurrents. We have shown the robustness of these findings against the presence of *e-e* interactions, providing insights into the study of correlation effects in 1D topological SCs with broken SIS. Finally, we introduced a supercurrent-assisted braiding of MZBSs, which has crucial applications to the realistic Majorana-fermion-based quantum computation. Interestingly, our results could be relevant to the emergence of a pseudo-Fermi surface resulted from the broken SIS and time-reversal symmetry in Z_2 spin liquids, explaining the intriguing properties observed in the organic compound $\mathrm{EtMe_3Sb[Pd(dmit)_2]_2}$.[50]

We thank K. Zuo, L. Kouwenhoven, Patrick A. Lee, H. Yao, M. Cheng, K. T. Law, C. Wang, and A. Iucci for helpful discussions. We acknowledge support from JQI-NSF-PFC, Microsoft-Q, and DARPA-QuEST.

[1] C. Nayak, S. H. Simon, A. Stern, M. Freedman, and S. Das Sarma, Rev. Mod. Phys. **80**, 1083 (2008).
[2] D. A. Ivanov, Phys. Rev. Lett. **86**, 268 (2001).
[3] S. Das Sarma, M. Freedman, and C. Nayak, Phys. Rev. Lett. **94**, 166802 (2005).
[4] N. Read and D. Green, Phys. Rev. B **61**, 10267 (2000).
[5] K. Sengupta, I. Žutić, H.-J. Kwon, V. M. Yakovenko, and S. Das Sarma, Phys. Rev. B **63**, 144531 (2001).
[6] A. Y. Kitaev, Phys. Usp. **44**, 131 (2001).
[7] L. Fu and C. L. Kane, Phys. Rev. Lett. **100**, 096407 (2008).
[8] J. Nilsson, A. R. Akhmerov, and C. W. J. Beenakker, Phys. Rev. Lett. **101**, 120403 (2008).
[9] J. Linder, Y. Tanaka, T. Yokoyama, A. Sudbø, and N. Nagaosa, Phys. Rev. Lett. **104**, 067001 (2010).
[10] J. D. Sau, R. M. Lutchyn, S. Tewari, and S. Das Sarma, Phys. Rev. Lett. **104**, 040502 (2010).
[11] J. Alicea, Phys. Rev. B **81**, 125318 (2010).
[12] R. M. Lutchyn, J. D. Sau, and S. Das Sarma, Phys. Rev. Lett. **105**, 077001 (2010).
[13] R. M. Lutchyn, T. D. Stanescu, and S. Das Sarma, Phys. Rev. Lett. **106**, 127001 (2011).
[14] T. D. Stanescu, R. M. Lutchyn, and S. Das Sarma, Phys. Rev. B **84**, 144522 (2011).
[15] Y. Oreg, G. Refael, and F. von Oppen, Phys. Rev. Lett. **105**, 177002 (2010).
[16] A. C. Potter and P. A. Lee, Phys. Rev. Lett. **105**, 227003 (2010).
[17] K. T. Law, P. A. Lee, and T. K. Ng, Phys. Rev. Lett. **103**, 237001 (2009).
[18] K. Flensberg, Phys. Rev. B **82**, 180516 (2010).
[19] M. Wimmer, A. R. Akhmerov, J. P. Dahlhaus, and C. W. J. Beenakker, New J. Phys. **13**, 053016 (2011).
[20] X.-J. Liu, Phys. Rev. Lett. **109**, 106404 (2012).
[21] C.-H. Lin, J. D. Sau, and S. Das Sarma, Phys. Rev. B **86**, 224511 (2012).
[22] V. Mourik, K. Zuo, S. M. Frolov, S. Plissard, E. A. Bakkers, and L. Kouwenhoven, Science **336**, 1003 (2012).
[23] M. T. Deng, C. L. Yu, G. Y. Huang, M. Larsson, P. Caroff, and H. Q. Xu, Nano Lett. **12**, 6414 (2012).
[24] A. Das, Y. Ronen, Y. Most, Y. Oreg, M. Heiblum, and H. Shtrikman, Nat. Phys. **8**, 887 (2012).
[25] A. Finck, D. V. Harlingen, P. Mohseni, K. Jung, and X. Li, arXiv:1212.1101v2.
[26] T. Giamarchi, *Quantum Physics in One Dimension* (Oxford University Press, Oxford, UK, 2004).
[27] M. Sato, Y. Takahashi, and S. Fujimoto, Phys. Rev. Lett. **103**, 020401 (2009).

[28]Note that the magnetic field orientation in the x-z plane which is perpendicular to the SO quantization axis, as considered by Jiang *et al.* (Ref. 29), cannot lead to the asymmetric dispersion relation.
[29]L. Jiang *et al.*, arXiv:1206.1581v1.
[30]The typical magnitude of θ_c may depend on materials. For InAs wire in proximity to the SC material Al and for parameters $\Delta_s \sim 40\ \mu$eV, $V_0 \sim 62.5\ \mu$eV, and $\mu \sim 0$ (cf. Ref. 24), it follows that $\theta_c \sim 0.22\pi$.
[31]M. Tinkham, *Introduction to Superconductivity*, 2nd ed. (McGraw-Hill, New York, 1996).
[32]J. D. McCambridge, Ph.D. thesis, Yale University, 1995.
[33]A. Romito, J. Alicea, G. Refael, and F. von Oppen, Phys. Rev. B **85**, 020502 (2012).
[34]See Supplemental Material at http://link.aps.org/supplemental/10.1103/PhysRevB.87.060504 for more details.
[35]X. G. Wen, Phys. Rev. B **41**, 12838 (1990).
[36]B. Blok and X. G. Wen, Phys. Rev. B **42**, 8133 (1990).
[37]V. I. Fernández, A. Iucci, and C. Naón, Eur. Phys. J. B **30**, 53 (2002).
[38]S. Gangadharaiah, B. Braunecker, P. Simon, and D. Loss, Phys. Rev. Lett. **107**, 036801 (2011).
[39]E. M. Stoudenmire, J. Alicea, O. A. Starykh, and M. P. A. Fisher, Phys. Rev. B **84**, 014503 (2011).
[40]L. Fidkowski, R. M. Lutchyn, C. Nayak, and M. P. A. Fisher, Phys. Rev. B **84**, 195436 (2011).
[41]A. M. Lobos, R. M. Lutchyn, and S. Das Sarma, Phys. Rev. Lett. **109**, 146403 (2012).
[42]J. Cardy, *Scaling and Renormalization in Statistical Physics* (Cambridge University Press, Cambridge, UK, 1996).
[43]G. I. Japaridze and A. A. Nersesyan, JETP Lett. **27**, 334 (1978).
[44]V. L. Pokrovsky and A. L. Talapov, Phys. Rev. Lett. **42**, 65 (1979).
[45]H. J. Schulz, Phys. Rev. B **22**, 5274 (1980).
[46]J. Alicea, Y. Oreg, G. Refael, F. von Oppen, and M. P. A. Fisher, Nat. Phys. **7**, 412 (2011).
[47]D. J. Clarke, J. D. Sau, and S. Tewari, Phys. Rev. B **84**, 035120 (2011).
[48]B. I. Halperin, Y. Oreg, A. Stern, G. Refael, J. Alicea, and F. von Oppen, Phys. Rev. B **85**, 144501 (2012).
[49]The orbital effects can generically harm the TQC. For example, for the type-II SC material NbTi to drive InSb nanowire deep into topological phase requires $B > 0.2$ T (Ref. 22), which is much larger than the lower critical field of NbTi (typically in the order of 10 mT). This effect complicates phase distribution of the induced SC order parameter in the Majorana network due to the formation of vortices in NbTi, and can lead to uncontrollable low-energy excitations in the network. For type-I SC, e.g., Al applying the $\boldsymbol{B}$ field out of plane may even destroy the SC phase since the critical field is typically very low.
[50]M. Barkeshli, H. Yao, and S. A. Kivelson, arXiv:1208.3869v1.